CONF-9606212--4

Novel Synthesis Process and Structure Refinements of $Li_4Mn_5O_{12}$ for Rechargeable Lithium Batteries

Toshimi Takada*, Hiroshi Hayakawa, and Etsuo Akiba

National Institute of Materials and Chemical Research

Higashi 1-1, Tsukuba, Ibaraki 305, Japan

Fujio Izumi

National Institute for Research in Inorganic Materials

Namiki 1-1, Tsukuba, Ibaraki 305, Japan

Bryan C. Chakoumakos

Oak Ridge National Laboratory **

P.O.Box 2008, Bldg 7962, Oak Ridge, Tennessee 37831-6393, U.S.A.

* To whom correspondence should be addressed.

**Managed by Lockheed Martin Energy Research Corp. under contract DE-AC05-96OR22464 for the U. S. Department of Energy.

ABSTRACT

Well crystallized $Li_4Mn_5O_{12}$ powder with grain size of 0.1 – 0.4 μm was prepared by heating a eutectic mixture of lithium acetate LiOAc, and manganese nitrate $Mn(NO_3)_2$, in an O_2 atmosphere. The structure of $Li_4Mn_5O_{12}$ crystallites was found to be cubic spinel using Rietveld refinement of both neutron and X-ray powder diffraction profiles. We confirmed that lithium ions occupy both the tetrahedral sites 8*a*, and part of the octahedral sites 16*d*, but not the 16*c* sites in the space group $Fd\bar{3}m$, while all the manganese ions occupy the 16*d* sites. The lattice parameter was found to be sensitive to synthesis temperature as a result of the variation in manganese valence. Sample prepared at 500°C showed better electrode performance. A rechargeable capacity of about 135 mAh/g for the cell $Li/Li_4Mn_5O_{12}$ was obtained in the range of cell voltages, 2.5 – 3.6 V.

Key Word: Spinel, Structure Refinement, Lithium Manganese Oxides, Rietveld Method, Lithium Batteries

DISCLAIMER

1. INTRODUCTION

Extensive research has been directed toward the development and optimization of the lithium manganese oxide electrode for rechargeable lithium batteries. Particular attention has been given to the spinels $LiMn_2O_4$, $Li_4Mn_5O_{12}$ and $Li_2Mn_4O_9$ (1–7). Currently, the spinel $Li[Li_xMn_{2-x}]O_4$ ($0.03<x<0.10$) is becoming more attractive because it shows better cycling performance. It is the current consensus that the wide range of solid solution exists within the Li-Mn-O family of spinel compounds, and the composition of the spinel electrode plays a very important role in controlling the rechargeability of the electrode (3). Therefore, attention should be paid to the control of the synthesis process to obtain single phase samples with the required stoichimetry. Understanding the crystal structural changes during the synthesis process is crucial for both process control and understanding the variation of the voltage, the capacity, and the cycling performance of Li/spinel cells.

In this study, we have focused on the synthesis process of well-crystallized $Li_4Mn_5O_{12}$, the confirmation of the cation distribution by neutron diffraction, and the structural changes caused by the presence of Mn^{3+}. The results of the structure refinements by the Rietveld method based on both X-ray and neutron powder diffraction data, and the preliminary results of the electrode performance of $Li/Li_4Mn_5O_{12}$ are presented.

2. EXPERIMENTAL

Synthesis of $Li_4Mn_5O_{12}$. 99.9% pure $LiOAc \cdot 2H_2O$ and $Mn(NO_3)_2 \cdot 6H_2O$ (from WAKO Pure Chemical Industries, Ltd.) were used as starting materials. Stoichiometric amounts of the raw materials were first heated at 100°C to obtain a uniform eutectic solution, and then slowly oxidized at 200°C under flowing O_2, thereby converting the eutectic solution to a solid Li-Mn-O precursor. Powder samples were obtained by heating the ground precursor at a temperature ranging from 400°C to 900°C for 1 – 3 days. All samples were heated at a rate of 100°C/hr and slowly cooled to room temperature in the furnace (about 7 hr) with 200

ml/min of flowing O_2. Details of the preparation process are described in our previous report (4).

X-ray diffraction. X-ray powder diffraction measurements were conducted at room temperature on a Rigaku RAX-I X-ray diffractometer with Cu-Kα radiation monochromated by a graphite single crystal at 40 kV, 30 mA. Data was collected between $2\theta = 15° - 120°$ with a step interval of 0.03.

Neutron diffraction. Neutron-diffraction data was collected using the HB4 high-resolution powder diffractometer at the High-Flux Isotope Reactor equipped with a Ge (115) monochromator at Oak Ridge National Laboratory (ORNL). The neutron wavelength was 1.4180(2). The sample (about 4.5g) was placed in a spinning vanadium can (1 cm I.D. by 6 cm) during data collection over the 2-theta range of 11° to 135° in steps of 0.05° at 295K. The structural refinements were carried out with the Rietveld-refinement program *RIETAN-94* (8, 9) on a Power Macintosh 8100/100AV.

Electrode Performance. The electrode performance of $Li_4Mn_5O_{12}$ was examined with a conventional electrochemical cell at room temperature, using Li metal as negative and reference electrode; 1.0 M $LiPF_6$ dissolved in ethylene carbonate (EC) and dimethyl carbonate (DMC) (1:1 in volume) as electrolyte. The composite electrode was made by mixing the $Li_4Mn_5O_{12}$ powder with 30.0 wt% acetylene black and 4.0 wt% of polyvinylidene fluoride (PVDF) dissolved in 1-methyl-2-pyrrolidone (NMP). The slurry was pressed onto an aluminum mesh current collector (10 × 10 mm square).

RESULT AND DISCUSSION

3.1 Synthesis of Well-Crystallized $Li_4Mn_5O_{12}$

Figure 1 shows the powder X-ray diffraction patterns of $Li_4Mn_5O_{12}$ prepared at 400°C, 500°C, 700°C and 800°C from LiOAc + $Mn(NO_3)_2$, and for comparison, the standard $LiMn_2O_4$ is also presented. Clearly, the higher reaction temperature gave the sharper and higher diffraction peaks, and consequently the

better crystallinity of $Li_4Mn_5O_{12}$. The minor monoclinic phase Li_2MnO_3, however, became apparent as the reaction temperature was raised above 700°C. The diffraction peaks of monoclinic phase Li_2MnO_3 in the sample obtained at 700°C and below were negligible. All the detected reflection peaks were consistent with that of a cubic spinel $LiMn_2O_4$, but with a visible shift to the higher 2θ / degree values corresponding to the contraction of the unit cell from a = 8.242Å for $LiMn_2O_4$ to 8.1610(5)Å for $Li_4Mn_5O_{12}$.

Figure 2 shows a typical SEM image of the $Li_4Mn_5O_{12}$ crystallites prepared at 700°C. Micrograph A for the sample prepared in powder form and B in pellet. Clearly, the size of $Li_4Mn_5O_{12}$ crystallites in these samples was uniformly distributed between 0.1 – 0.4 μm. The uniformity in the size and shape of the crystallites as shown by micrographs A and B could be a results of the homogeneity of the Li-Mn-O precursor.

3.2 Structural Refinement of $Li_4Mn_5O_{12}$ by the Rietveld Method

Refinements were initiated in the space group $Fd\bar{3}m$ using the initial structural model with atomic coordinates from our previous X-ray diffraction study of $Li_4Mn_5O_{12}$ (4). The following neutron scattering lengths were used: b_{Li} = -0.1900 × 10^{-14} m, b_{Mn} = -0.3730 × 10^{-14} m, b_O = 0.5803 × 10^{-14} m. The simultaneous refinement was carried out on two crystalline phases: $Li_4Mn_5O_{12}$ (space group $Fd\bar{3}m$., No. 227) and Li_2MnO_3 ($C2/m$, No. 12). The crystallographic parameters of Li_2MnO_3 were adopted from Strobel and Andron (Ref.10). Only the scale factor and cell parameters for Li_2MnO_3 were refined because of its small content (<5%). To obtain better consistency in the crystallographic data for $Li_4Mn_5O_{12}$, several constraints were applied to these refinements at final stages. The site occupancy of the octahedrally-coordinated manganese ions in the 16*d* sites was finally refined based on the X-ray diffraction data because manganese is more sensitive to X-ray, while the occupancy of Li in the 8*a* sites and oxygen in the 32*e* sites, and overall isotropic thermal parameters were determined using the neutron diffraction data. The final observed, calculated, and difference profiles are shown

in Fig. 3 and the refined lattice parameter, atomic coordinates, and thermal parameters for $Li_4Mn_5O_{12}$ prepared at 700°C are listed in Table 1.

The site occupancies confirmed that the ion distribution is very close to the ideal arrangement, $(Li)_{8a}[Li_{1/3}Mn_{5/3}]_{16d}O_4$. The occupation of the interstitial 16*c* sites by Li and the 8*a* sites by Mn are ruled out. Allowing variation of the oxygen site occupancy factor results in a value of 1.0 within the standard deviation, which indicates that the oxygen is very nearly stoichimetric in this sample. Instead, the occupancy of manganese in the 16d sites, q_{Mn}, is found to be 0.84, with an estimated standard deviation (e.s.d.) of 0.02. The value of q_{Mn} is a little higher but in good agreement with 0.833 for the ideal arrangement of $Li_4Mn_5O_{12}$, in which 0.333 Li ions are required to compensate the imbalance in charge in the 16*d* sites assuming all the manganese ions are in the 4+ state. From the point of view of electroneutrality, a higher value of q_{Mn} indicates the presence of Mn^{3+} ions.

3.3 Structural changes of $Li_4Mn_5O_{12}$ with Synthesis Temperatures

Analogous refinement of the data for a sample prepared at low temperature resulted in similar crystallographic parameters. The crystallographic parameters for the sample prepared at 500°C are almost identical to that of the sample prepared at 700°C, except for the lattice parameter a = 8.1405(10)Å. It means about 0.7% contraction in volume of the unit cell from the sample prepared at 700°C. The refined site occupancy of manganese in the 16d sites, q_{Mn}, is 0.83±0.01 which is identical to 0.833 of the ideal arrangement, indicating that the oxidation state of manganese in this sample is very close to 4+.

Refinement of manganese site occupancy factor revealed that q_{Mn} increased with synthesis temperature. The refined q_{Mn} for spinel Li-Mn-O, and the portion of precipitated Li_2MnO_3 in the final product are plotted in Fig. 4 against the synthesis temperature, along with the lattice parameter. As the synthesis temperature was raised to 900°C, the site occupancy q_{Mn}, reached 1.0, which indicates a changes in the composition of the spinel phase. Since no evidence for oxygen deficiency in the 32*e* sites was found in these refinements, the spinel phase

should be stoichiometric with a composition, lying on the tie line between $Li_4Mn_5O_{12}$ and $LiMn_2O_4$ in the Li-Mn-O diagram (2, 3), which can be simply expressed as $Li_{1+x}Mn_{2-x}O_4$ ($1/3 \leq x \leq 0$). The compositional change of the spinel from $Li_4Mn_5O_{12}$ to $LiMn_2O_4$, thus, can be expressed as:

$$Li_4Mn_5O_{12} \xrightarrow{>700^\circ C \text{ in } O_2} \alpha\, Li[Li_xMn_{2-x}]O_4 + \beta\, Li_2MnO_3 + \varepsilon\, O_2\uparrow \quad [1].$$

As temperature increases, x decreases from 1/3 to 0, the lithium ions in the octahedral 16*d* sites are replaced by Mn^{3+} ions. Therefore, the increase of the lattice parameter with synthesis temperature can be easily ascribed to the presence of larger Mn^{3+} ions in the samples prepared at elevated temperatures. The effective ion radii of octahedrally coordinated Mn^{3+} and Mn^{4+}, are 0.645 (at high spin state) and 0.56Å, respectively. The precipitation of Li_2MnO_3, thus, occurs to consume the excess Li. Details of this transition was discussed separately (6).

3.3 Electrode Performance of $Li_4Mn_5O_{12}$

The cyclic voltammograms between 1.5 and 4.6 V swept at 1.0 mA/s are shown in Fig. 5 for $Li/Li_4Mn_5O_{12}$ cells. The sample prepared at 500°C showed a larger peak around 2.6 V but smaller one at 3.9 V than those of 700°C sample. Theoretically, $Li_4Mn_5O_{12}$ offers no capacity at 4.0 V region because the manganese ions are tetravalent and it is not possible to oxidize these cations further by electrochemical extraction of lithium at practical voltages (< 5.0 V). Therefore, the peak around 3.9 V indicates that the manganese valence should be less than 4.0, thus, a portion of Mn^{3+} ions was existed in these samples. Larger peak at 3.9 V reveals that larger portion of the Mn^{3+} ions exists in the sample prepared at higher temperature. This is in good agreement with the results of Rietveld refinements.

Figures 6 (a) and (b) show the initial 10 charge and discharge profiles of two $Li/Li_4Mn_5O_{12}$ cells, when cycled between voltage limits of 2.5 V and 3.6 V, at a current density of 0.3 mA/cm^2. The cycle performance was shown in Figure 6 (c) and (d), respectively, given in the cathode capacity delivered per cycle, calculated on the mass of the active material only. The active materials synthesized at 500°C and 700°C show similar charge/discharge profiles around 2.9 V. The cell using the

sample synthesized at 700°C showed a much lower capacity and a continuous decrease in capacity with cycling from 100 to 76 mAh/g after the initial 10 cycles. While the cell using the sample synthesized at 500°C showed better capacity retention and delivered over 100 mAh/g after initial 10 cycles. Consequently, the manganese valence in $Li_4Mn_5O_{12}$ has a profound effect on the electrode performance of Li/$Li_4Mn_5O_{12}$ cell. Synthesis of $Li_4Mn_5O_{12}$ with all manganese ions in the 4.0+ oxidation state is crucial to obtain good electrode performance.

CONCLUSION

Well crystallized $Li_4Mn_5O_{12}$ has been prepared from the eutectic of LiOAc and $Mn(NO_3)_2$ under flowing oxygen. Rietveld refinement with X-ray and neutron powder diffraction data indicated that $Li_4Mn_5O_{12}$ possesses a cubic spinel structure, in which, lithium ions occupy both the tetrahedral sites 8*a* , and part of the octahedral sites 16*d*, but not the 16*c* sites, while all the manganese ions occupy the 16*d* sites of the space group $Fd\bar{3}m$. The lattice parameter was found to be sensitive to the synthesis temperature as a result of the variation in manganese valence. Sample prepared at 500°C showed better electrode performance; a rechargeable capacity of about 135 mAh/g for the cell Li/$Li_4Mn_5O_{12}$ in the range of cell voltages 2.5 – 3.6 V. It is found that the oxidation state of manganese in $Li_4Mn_5O_{12}$ has a strong effect on the electrode performance of Li/ $Li_4Mn_5O_{12}$ cell.

ACKNOWLEDGMENT

The authors would like to thank A. Goto, Dr. M. Yoshikawa, Hitachi, Ltd, and Dr. T. Horiba, Shin-Kobe Electric Machinery Co., Ltd, for performing the electrochemical measurements. The neutron diffraction work was conducted at Oak Ridge National Laboratory which is managed by Lockheed Martin Energy Research for the U.S. Department of Energy under contract number DE-AC05-96OR22464.

List of the Figure and Table Caption

Fig. 1. X-ray diffraction patterns for $Li_4Mn_5O_{12}$ prepared at temperatures ranging from 400°C to 800°C under flowing oxygen using LiOAc and $Mn(NO_3)_2$ as raw materials, for comparison that of $LiMn_2O_4$ is presented. Arrows indicate the reflections from Li_2MnO_3.

Fig. 2. Scanning electron micrographs of the $Li_4Mn_5O_{12}$ crystallites prepared at 700°C, A in powder form and B in pellet.

Fig. 3. Rietveld refinement profiles for the $Li_4Mn_5O_{12}$ sample prepared at 700°C. Observed (dots) and calculated (solid line) intensities are shown at the top, and difference of the observed and calculated intensities (ΔI) at the bottom. The tick marks below the pattern indicate the positions of all possible Bragg reflections from $Li_4Mn_5O_{12}$ (upper) and Li_2MnO_3 (lower). R factors as defined in Ref.9 are given for reference.

Fig. 4. Plot of the refined q_{Mn}, the portion of precipitated Li_2MnO_3 against the synthesis temperature, along with the lattice parameter for spinel Li-Mn-O.

Fig. 5. Cyclic voltammograms within the 1.5 to 4.6 V potential range for $Li/Li_4Mn_5O_{12}$ cells using samples prepared at 500°C and 700°C, respectively.

Fig. 6. Charge/discharge profiles for the initial 10 cycles of $Li/Li_4Mn_5O_{12}$ cells using powder samples synthesized at 500°C and 700°C, respectively, for (a) and (b). The capacity delivered per cycle for these cells is shown in the corresponding figures below (c) and (d).

Table 1. Crystallographic parameters of $Li_4Mn_5O_{12}$ prepared from LiOAc and $Mn(NO_3)_2$ at 700°C under flowing oxygen.

REFERENCES

1. J. M. Tarascon, W. R. McKinnon, F. Coowar, T. N. Bowmer, G. Amatucci, and D. Guyomard, *J. Electrochem. Soc.* **141**(6), 1421 (1994).
2. R. J. Gummow, A. de Kock, and M. M. Thackeray, *Solid State Ionics* **69**, 59 (1994).
3. M. M.Thackeray, M.F. Mansuetto, D.W.Dees, and D.R.Vissers, *Mater. Res. Bull.* **31** (2), 133 (1996).
4. T. Takada, H. Hayakawa, and E. Akiba,*J. Solid State Chem.* **115**, 420 (1995).
5. T. Takada, H. Hayakawa, T. Kumagai, and E. Akiba, *J. Solid State Chem.* **121**, 79 (1996).
6. T. Takada, H. Hayakawa, E. Akiba, F. Izumi, and B. Chakoumakos, *J. Solid State Chem.*, **submitted.**
7. M. N. Richard, E. W. Fuller, and J. R. Dahn, *Solid State Ionics* **73**, 81 (1994).
8. F. Izumi, in *"The Rietveld Method"* edited by R. A. Young, pp. 236-253, Oxford University Press Inc., New York, 1993.
9. R. A. Young, *"The Rietveld Method"* , Oxford University Press Inc., New York, 1993.
10. P. Strobel and B. Lambert-Andron, *J. Solid state chem.* , **75**, 90, (1988).

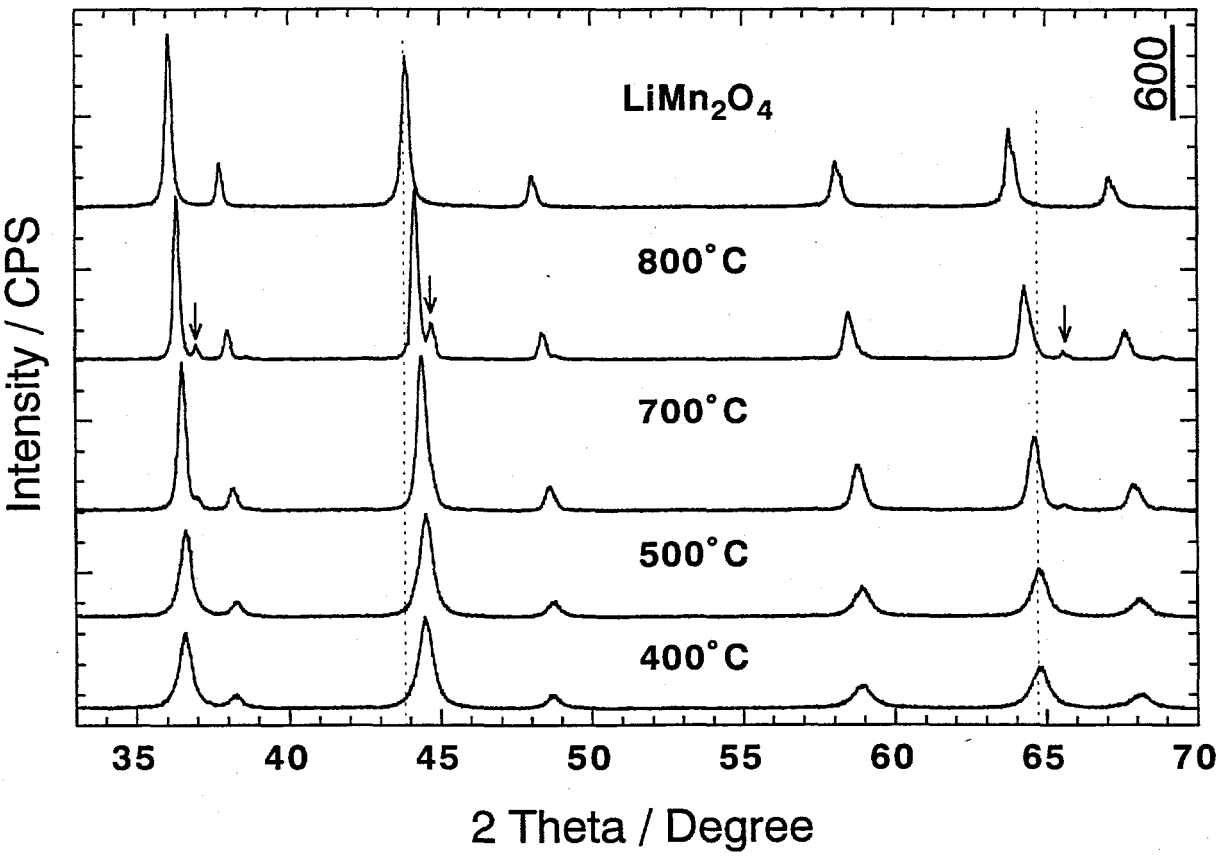

Fig. 1

takada et al.

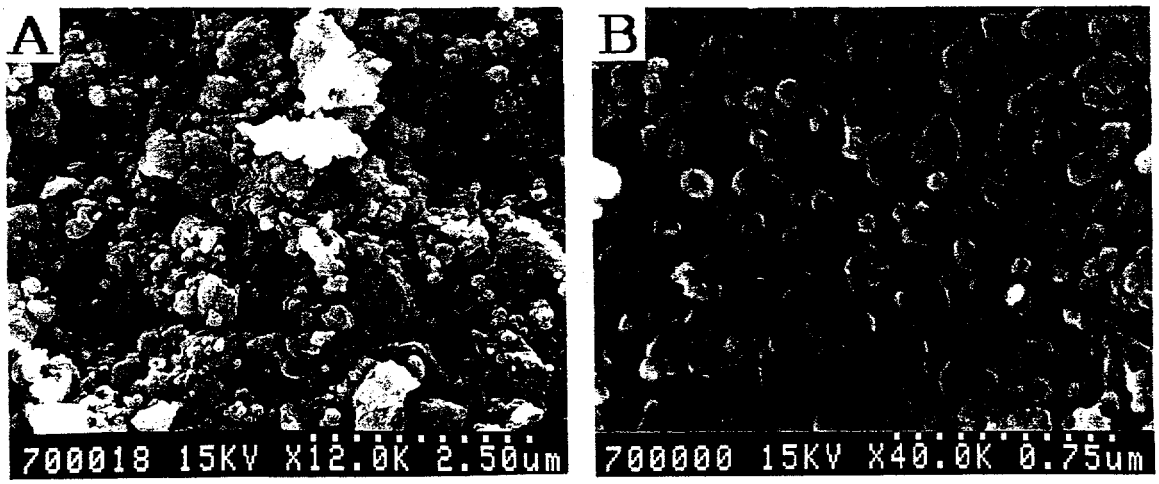

Fig. 2

Takada et al.

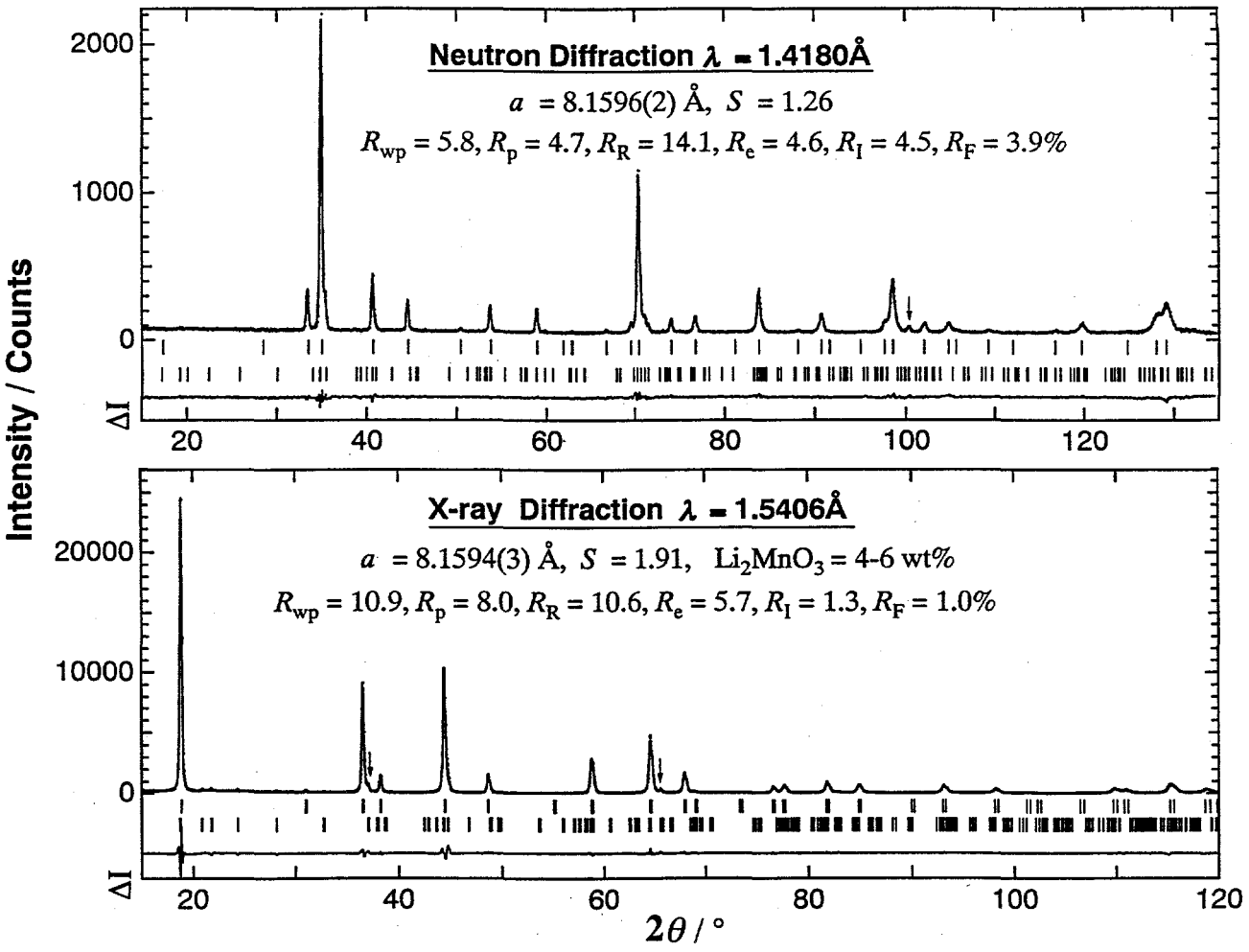

FIG. 3

takada et al.

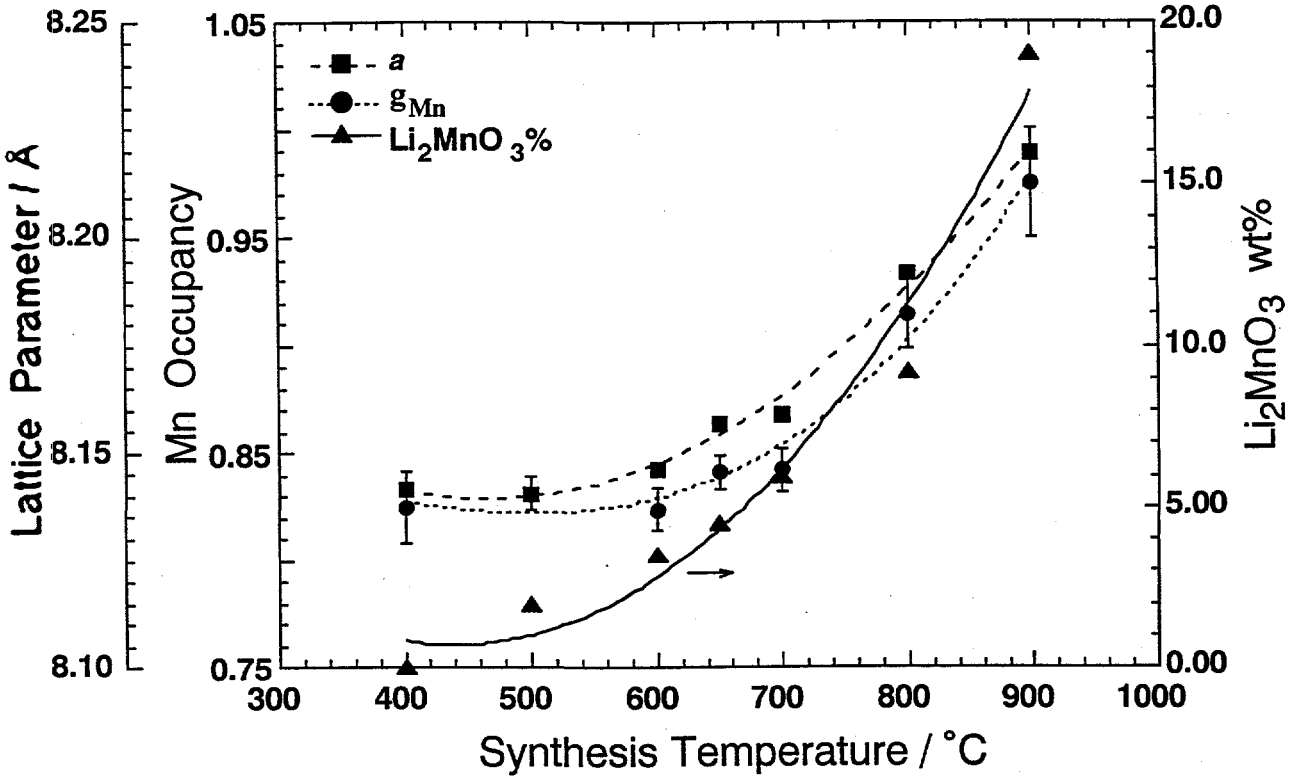

FIG. 4

takada et al.

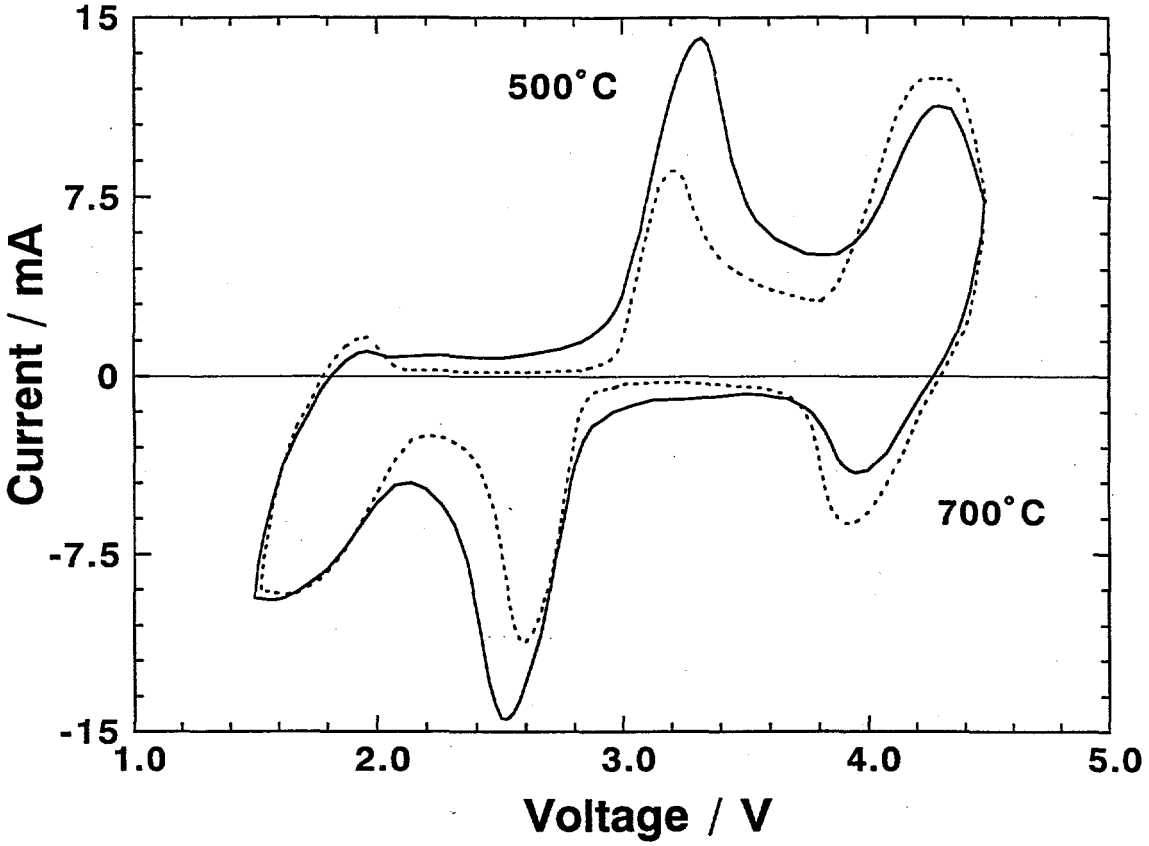

Fig. 5

Takada et al.

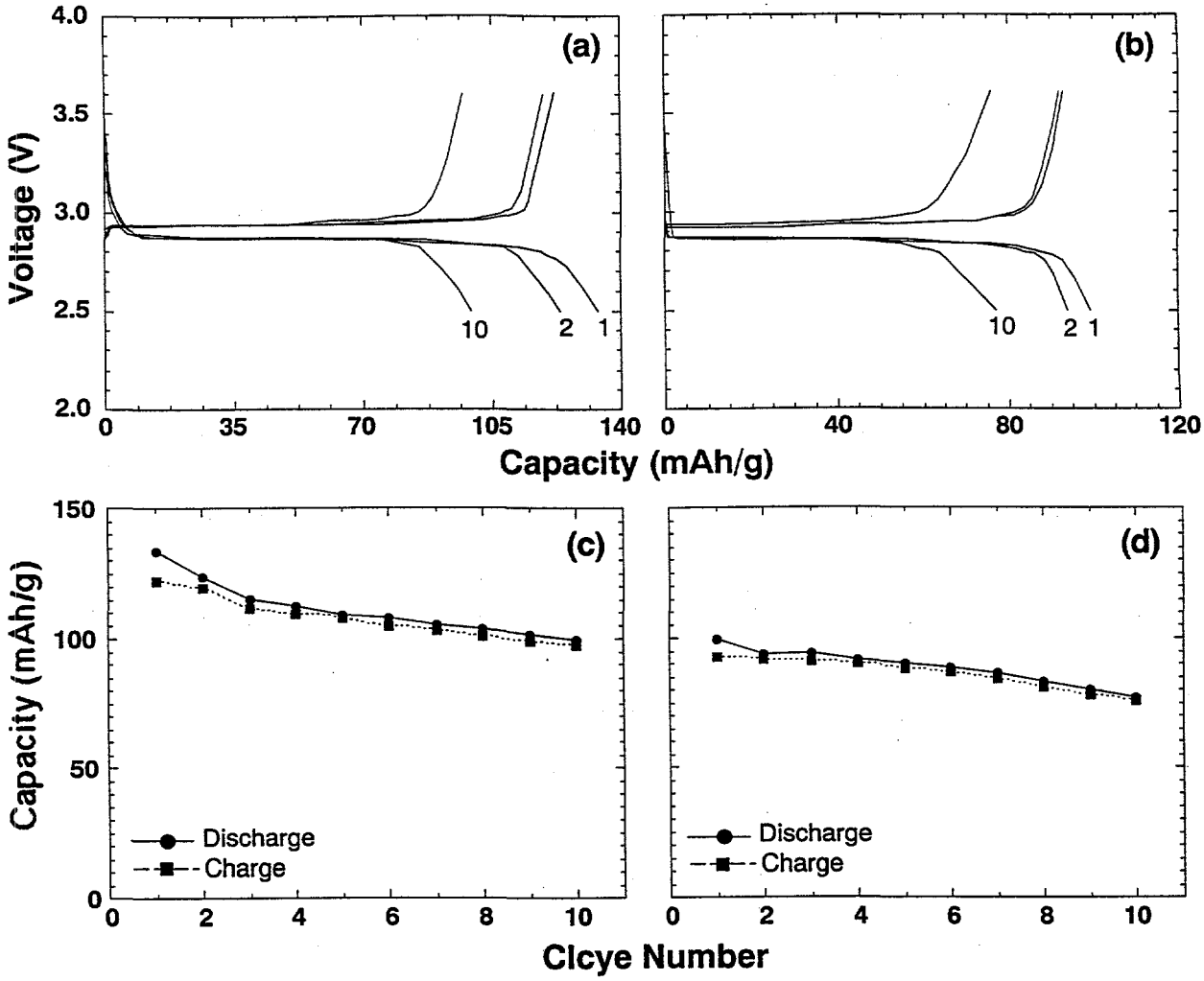

Fig.6

Takada et al.

Table 1. Crystallographic parameters of $Li_4Mn_5O_{12}$ prepared from LiOAc and $Mn(NO_3)_2$ at 700° C under flowing oxygen.

Space group: $Fd\bar{3}m$, No.227 $a^x = 8.1594(3)$Å, $a^n = 8.1596(2)$Å				
Atom	**site**	***x = y = z***	***g***	***B* (Å²)**
Li(1)	8*a*	0.0	1.00(5)^n	1.0 (2)^n
Li(2)[a]	16*d*	0.625	0.16	= B_{Mn}
Mn	16*d*	0.625	0.84(2)^x	0.40(5)^x
O	32*e*	0.3878(3)^x 0.3880(1)^n	1.00(2)^n	0.80(4)^n

All numbers in the parentheses present the e.s.d. to the left.
g is the site occupancy.

[a] - Constrains on the site occupancy $g_{Mn} + g_{Li(2)} = 1$ and isotropic thermal parameter $B_{Mn} = B_{Li(2)}$ were applied.

[x]- Parameters that refined from X-ray diffraction data

[n] - Parameters that refined from neutron diffraction data

Takada et. al